DOI: 10.1002/cbic.201000486

Heparin Inhibits Membrane Interactions and Lipid-Induced Fibrillation of a Prion Amyloidogenic Determinant

Ehud Bazar, Tania Sheynis, Jerzy Dorosz, and Raz Jelinek*[a]

Glycosaminoglycans (GAGs), particularly heparin, are known to reduce the toxicities of various amyloidogenic proteins. The molecular factors underlying the antitoxic effects of GAGs, however, are still not fully understood. Because interactions of amyloidogenic proteins and their aggregates with membranes are believed to play major roles in affecting amyloid pathogenesis, our objective in this study was to elucidate the effect of heparin on membrane interactions of the 21-residue amyloidogenic determinant of the prion protein [PrP(106–126)]. Indeed, the experimental results indicate that heparin significantly interferes in membrane interactions of the prion peptide. Specifically, we show that there is direct competition for binding of PrP(106–126) between heparin on the one hand and negatively charged phospholipids on the other hand. The data reveal that heparin, even in very low molar concentrations, exhibited high affinity towards PrP(106–126) and consequently suppressed interactions of the peptide with lipid vesicles. Interestingly, whereas heparin significantly inhibited lipid-induced PrP(106–126) fibrillation, it still promoted fibril formation in aqueous solutions independently of the lipid vesicles present. Our results strongly suggest that the primary effects of GAGs in attenuating amyloid toxicities are due to blocking of membrane interactions of the amyloidogenic proteins rather than modulation of their fibrillation properties.

Introduction

Prion diseases encompass several devastating neurological conditions, believed to be caused by infectious misfolded protein species.[1] The primary pathological feature of prion diseases is the conversion of the normal cellular prion protein (PrP^C) into the aberrant isoform (PrP^{Sc}) in a post-translational process involving significant secondary structural changes.[2] The abnormal, protease-resistant isoform is rich in β-sheet structure and aggregates into amyloid fibrils or plaques found in endosomes, lysosomes, on the cell surface,[3] and in extracellular spaces.[4]

Previous reports noted that PrP^C is preferentially located in the cell membrane, due to its glycosylphosphatidylinositol (GPI) anchor.[5] Indeed, membrane surfaces are believed to be intimately involved in the conversion of PrP^C into PrP^{Sc}, and interactions of PrP with the plasma membrane might be a critical component in the mechanism of prion toxicity.[6] In a broader context, lipid and membrane interactions of amyloidogenic proteins appear to play pivotal roles in the pathologies of many amyloid diseases.[7,8] In particular, lipid bilayers have been shown to constitute targets for docking of amyloid protein aggregates.[9] Lipids and lipid assemblies also promote fibrillation of various amyloid protein species.[9–11]

Glycosaminoglycans (GAGs), negatively charged polysaccharides abundant in the extracellular matrix, have been shown to associate with different types of amyloid deposits, including PrP^{Sc}.[12–15] The precise roles of GAGs in amyloidogenesis is debated, but several studies have reported that GAGs caused a *reduction* in mortality of amyloid-infected cells.[16–20] GAGs, particularly heparin, are also known to act as effective modulators of fibrillation processes.[18,21–23] We have recently shown that heparin induced dramatically divergent concentration-dependent fibrillation pathways for the amyloidogenic determinant of the prion protein.[24]

For better understanding of the influence of GAGs upon amyloidogenic proteins, we present here an investigation of the relationship between heparin binding and membrane interactions of a peptide fragment spanning residues 106–126 of the prion protein [PrP(106–126)]. PrP(106–126) has been widely studied as a surrogate of the full-length prion[25] because its neurotoxic activity and fibrillation properties are similar to those of the full-length prion protein.[18,26–28] Although previous studies have focused on the effects of lipids and membranes upon PrP(106–126)[29,30] or the reciprocal impact of the prion peptide on lipid bilayers,[31–35] no comprehensive, unified analysis has examined the relationship between heparin and membrane interactions of PrP(106–126).

In a broader context, shedding light on the interplay between membrane interactions of amyloidogenic peptides and the effect of GAGs (or other fibrillation modulators) is a critical component in elucidating the complex physiological scenarios underlying the devastating outcome of amyloid diseases. Furthermore, elucidating and understanding of the antitoxic properties of GAGs in amyloid systems could aid in identifying potential therapeutic pathways for combating these diseases.

[a] *E. Bazar, Dr. T. Sheynis, Dr. J. Dorosz, Prof. R. Jelinek*
Department of Chemistry, Ben Gurion University of the Negev
Beer Sheva 84105 (Israel)
Fax: (+972) 8-647-2943
E-mail: razj@bgu.ac.il

Results

The experiments presented here were designed to investigate the interplay between the effects of *lipid bilayers* versus *heparin* both on the structural transformations and aggregation of PrP(106–126) and on the membrane interactions of the peptide. Figure 1 examines the effects of phospholipid vesicles and of heparin/vesicle mixtures on the fibrillation kinetics of PrP(106–126). The experiments in Figure 1 A compare the fibrillation of PrP(106–126) in the presence of vesicles consisting of *zwitterionic* phospholipids (dimirystoylphosphatydilcholine, DMPC) with that of vesicles containing a mixture of DMPC and *negatively charged* dimirystoylphosphatydilglycerol (DMPG). The fluorescence curves of thioflavin-T (ThT), a dye that binds to fibrillar structures and is commonly used as a marker for fibril formation,[36] clearly illuminate the dramatic effect of DMPG in promoting PrP fibrillation (Figure 1 A). Specifically, virtually no increase in ThT fluorescence was recorded when PrP(106–126) was dissolved in an aqueous buffer solution (Figure 1 A, i) or in the presence of DMPC vesicles (Figure 1 A, ii). In contrast, a significant increase in ThT fluorescence, indicating rapid fibrillation, was apparent within few minutes after PrP(106–126) was placed in an aqueous solution containing DMPC/***DMPG*** vesicles (Figure 1 A, iii).

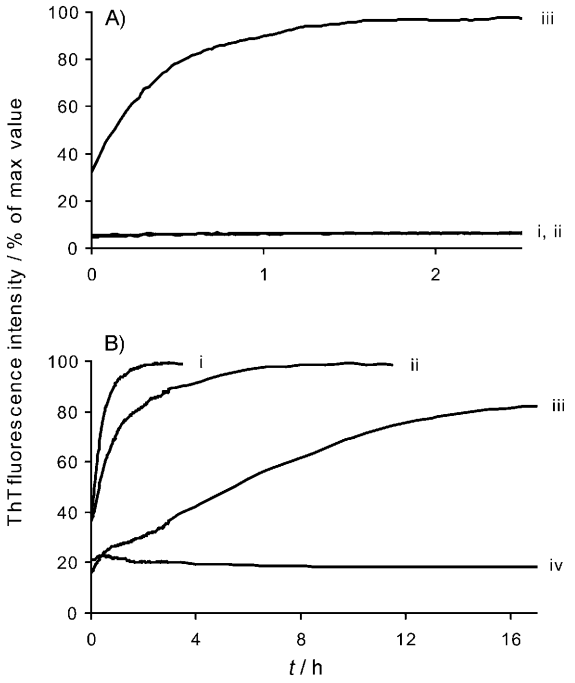

Figure 1. Fibrillation of PrP(106–126) is significantly modulated by negatively charged phospholipids and by heparin. ThT fluorescence curves were recorded in solutions containing: A) i: PrP(106–126) in buffer, ii: PrP(106–126) added to DMPC vesicles, and iii: PrP(106–126) added to DMPC/DMPG vesicles, or B) i: PrP(106–126) added to DMPC/DMPG vesicles, ii: *heparin* + PrP(106–126) [0.2:1 weight ratio between heparin and PrP(106–126)] added to DMPC/DMPG vesicles, iii: *heparin* + PrP(106–126) [1:1 weight ratio between heparin and PrP(106–126)] added to DMPC/DMPG vesicles, and iv: *heparin* + PrP(106–126) [5:1 weight ratio between heparin and PrP(106–126)] added to DMPC/DMPG vesicles.

The effect of *heparin* upon PrP(106–126) fibrillation in solutions containing both the peptide *and* DMPC/DMPG vesicles is depicted in Figure 1 B, and the corresponding aggregation constants (k_{agg}) calculated through exponential curve fitting[37] are outlined in Table 1. Both the ThT fluorescence curves in Figure 1 B and the k_{agg} values in Table 1 demonstrate that the fibrillation process of PrP(106–126) was intimately modulated by heparin. Specifically, the addition of heparin significantly *retarded* fibril formation of PrP(106–126) (Figure 1 B, ii–iv).

Table 1. Aggregation rate constants (k_{agg}) for PrP(106–126); k_{agg} values were calculated through exponential curve fitting.[37]

Heparin PrP(106–126) weight ratio	$k_{agg} \times 10^{-4}$ [s^{-1}] in buffer[24]	$k_{agg} \times 10^{-4}$ [s^{-1}] in the presence of DMPC/PCPG vesicles
0	negligible fibrillation	11.2 ± 0.6
0.2:1	4.5 ± 0.1	5.5 ± 0.3
1:1	0.56 ± 0.04	0.74 ± 0.04
5:1	negligible fibrillation	negligible fibrillation

Particularly notably, Figure 1 B and Table 1 indicate that the extent of fibrillation of PrP(106–126) was dependent upon the *mole ratio* between heparin and PrP(106–126). In a DMPC/DMPG vesicle solution not containing heparin, PrP(106–126) exhibited rapid aggregation (k_{agg} of $11.2 \times 10^{-4}\ s^{-1}$, Table 1). A *low* heparin concentration [0.2:1 weight ratio between heparin and PrP(106–126), Figure 1 B, ii] resulted in a lower rate of fibrillation (k_{agg} of $5.5 \times 10^{-4}\ s^{-1}$, Table 1). A significantly *slower* PrP(106–126) fibrillation rate was apparent when the concentration of heparin was increased: in a solution containing a 1:1 weight ratio between heparin and PrP(106–126) (Figure 1 B, iii), for example, the calculated k_{agg} value was $0.74 \times 10^{-4}\ s^{-1}$. Negligible PrP(106–126) fibrillation occurred when a very high concentration of heparin was present in the peptide/vesicle solution [5:1 weight ratio between heparin and PrP(106–126), Figure 1 B, iv].

The ThT fluorescence data in Figure 1 B demonstrate that heparin interfered with lipid-induced fibrillation of PrP(106–126), significantly modulating the kinetic profile of the fibrillation process. Specifically, *enhanced* PrP(106–126) fibrillation occurred in a solution of *low* mole ratio between heparin and the prion peptide, whereas *inhibition* of peptide aggregation was observed when the heparin/PrP(106–126) ratio was high. Importantly, the pronounced dependence of PrP(106–126) fibrillation upon the heparin/PrP(106–126) mole ratios almost exactly echoes the effect of heparin upon PrP(106–126) fibrillation in *vesicle-free* solutions.[24] Specifically, the calculated k_{agg} values for the heparin/DMPC/DMPG mixtures shown in Table 1 appear highly similar to the values recently reported in the case of PrP(106–126)/heparin solutions *not containing* DMPC/DMPG vesicles.[24] Accordingly, the ThT data in Figure 1 B suggest that heparin essentially "masks" the vesicle membrane, reducing or eliminating the electrostatic attraction between the negatively charged phospholipids and the prion peptide. As a consequence, *heparin* rather than the *DMPC/DMPG vesicles*

constituted the determining factor for the PrP(106–126) fibrillation kinetics.

To corroborate this interpretation and to determine the extent to which heparin indeed interferes with membrane interactions of PrP(106–126), we applied several biophysical techniques, including Langmuir monolayer analysis (Figure 2),

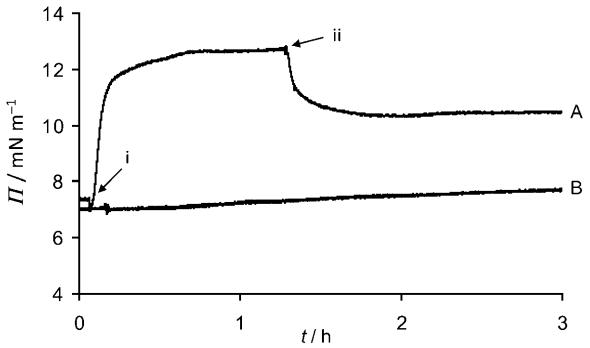

Figure 2. PrP(106–126) binds to DMPC/DMPG Langmuir monolayers, but heparin inhibited monolayer attachment of the prion peptide. Adsorption isotherms were measured by use of DMPC/DMPG monolayers (1:1 mole ratio) at an initial surface pressure of around 7 mN m^{-1}. A) i: PrP(106–126) was injected into the water subphase (0.5 μM), and ii: subsequently heparin (0.0125 mg mL^{-1}) was injected. B) PrP(106–126) was injected into the water subphase *already containing* heparin (0.005 mg mL^{-1})

fluorescence resonance energy transfer (FRET, Figure 3, below), circular dichroism (CD, Figure 4, below), and transmission electron microscopy (TEM, Figure 5, below). Figure 2 depicts monolayer adsorption experiments designed to evaluate the affinity of PrP(106–126) to lipid surfaces and the effect of heparin upon prion–lipid interactions. Langmuir lipid monolayers have often been used to mimic bilayer surfaces and the membrane/water interface.[38] In particular, Langmuir experiments facilitate analysis of the thermodynamic parameters pertaining to lipid adsorption of membrane-active molecules.[39]

Figure 2 depicts adsorption isotherms recorded in a Langmuir trough in which a DMPC/DMPG monolayer (1:1 mole ratio) was spread upon the water subphase. After deposition, the phospholipid monolayer gave rise to a constant surface pressure of approximately 7 mN m^{-1}. The adsorption isotherm in Figure 2 A clearly shows that when PrP(106–126) was injected into the water subphase underneath the DMPG/DMPG monolayer, a rapid increase in surface pressure was recorded (Figure 2 A, i), reflecting the high affinity of the prion peptide towards the negatively charged phospholipids.[29] The dramatic effect of heparin upon binding of PrP(106–126) to the DMPC/DMPG monolayer is apparent in Figure 2 A, ii—in which a pronounced decrease in surface pressure occurred immediately after heparin was inserted into the water subphase. This result indicates that PrP(106–126) attraction to the water-soluble *heparin* largely overcame its affinity to the *DMPG/DMPG* monolayer, effectively detaching the peptide from the monolayer and thereby reducing the surface pressure.

The adsorption isotherm in Figure 2 B provides further evidence for the inhibition effect of heparin on PrP(106–126) binding to negatively charged phospholipids. Indeed, hardly any increase in surface pressure was recorded when PrP(106–126) was injected into a water subphase solution that *already contained* heparin (Figure 2 B). This result confirms that heparin effectively blocked PrP(106–126) association with the lipid monolayer.

Whereas the adsorption isotherm experiments in Figure 2 highlight heparin-induced inhibition of PrP(106–126) binding to negatively charged phospholipids, we further analyzed how heparin affected the disruption of *phospholipid vesicles* by PrP(106–126) (Figure 3). In general, lipid vesicles better mimic the *bilayer* environments of cellular membranes. The bar diagram in Figure 3 depicts the results of a fluorescence reso-

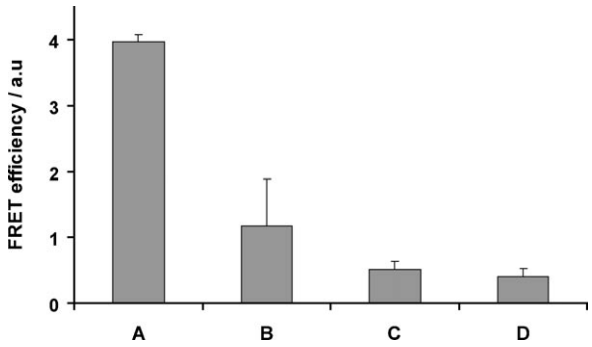

Figure 3. Heparin inhibits FRET enhancement induced by interactions of PrP(106–126) with NBD-PE/Rh-PE/DMPC/DMPG vesicles. Increased FRET efficiencies were recorded in NBD-PE/Rh-PE/DMPC/DMPG vesicles (1:1:100:100 mole ratio) after addition of PrP(106–126) and heparin in different concentrations (*zero* FRET efficiency is defined as the energy transfer recorded in the vesicles prior to addition of the peptide/heparin): A) only PrP(106–126) (no heparin), B) *0.2:1* weight ratio between heparin and PrP(106–126), C) *1:1* weight ratio between heparin and PrP(106–126), and D) *5:1* weight ratio between heparin and PrP(106–126).

nance energy transfer (FRET) experiment employing DMPC/DMPG vesicles that further contained the lipid dyes NBD-PE (fluorescence donor) and Rh-PE (fluorescence acceptor). FRET experiments employing dye-containing vesicles have been widely used to evaluate lipid interactions and bilayer disruption by membrane-active species.[40]

Figure 3 reveals both the significant effect of PrP(106–126) on lipid bilayers, as well as the attenuation of the bilayer interactions of the prion peptide by heparin. Figure 3 A shows that incubation of PrP(106–126) with NBD-PE/Rh-PE/DMPC/DMPG vesicles resulted in a pronounced *increase* in FRET efficiency. This effect has not been widely observed for membrane-active peptides (which generally result in *reduction* of FRET efficiency in vesicles containing fluorescence donors and acceptors), and is ascribed to aggregation of the vesicles by the assembled prion fibrils.[41] Essentially, we believe that the PrP fibrillation occurs in close proximity to the lipid bilayer surface, effectively immobilizing the bilayer constituents, particularly the fluorescence donors and acceptors, thus facilitating enhanced energy transfer among them. A similar FRET enhancement effect was recently reported in the case of lipid-induced fibrillation of calcitonin fragments.[42]

The significant inhibition effect of heparin upon vesicle interactions of PrP(106–126) is apparent in the FRET results shown in Figure 3B–D. Essentially, the presence of heparin in the vesicle solutions resulted in *lower* FRET efficiencies, approaching the FRET values of the control vesicles not treated with PrP(106–126) (Figure 3B–D). This experimental outcome indicates that heparin effectively prevented binding of the prion fragment to the DMPC/DMPG vesicles. Similarly to the ThT data in Figure 1B above, the concentration-dependent decrease in FRET efficiency in Figure 3 underscores the close relationship between the effect of heparin upon PrP(106–126) fibrillation and the mole ratio between heparin and the prion peptide.

To gain insight into the *structural effects* of heparin upon PrP(106–126) in lipid vesicle solutions we applied CD spectroscopy (Figure 4). Figure 4 depicts the CD signatures of PrP(106–126) added to solutions consisting of DMPC/DMPG vesicles and heparin at different mole ratios. In the presence of DMPC/DMPG vesicles but *without* heparin, PrP(106–126) adopted a β-sheet conformation, reflected in the shallow spectral well around 220 nm and the positive signal at 195 nm (Figure 4, i).[43] A β-sheet structure of PrP(106–126) was still observed when the solution contained heparin and PrP(106–126) at a weight ratio of 0.2:1 (Figure 4, ii). Higher concentrations of heparin, however, significantly reduced the abundance of β-sheet peptide conformation (Figure 4, iii–iv), eventually giving rise to a random coil structure in a solution containing heparin and PrP(106-126) at a 5:1 weight ratio (Figure 4, iv).

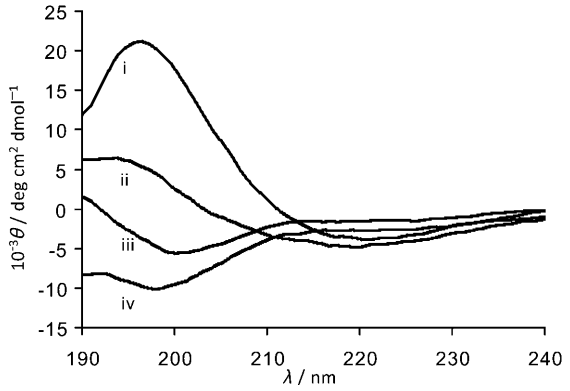

Figure 4. Heparin inhibits vesicle-induced β-sheet formation in PrP(106–126). Circular dichroism CD spectra of PrP(106–126) incubated with DMPC/DMPG vesicles (1:1 mole ratio). i: no heparin added, ii: 0.2:1 weight ratio between heparin and PrP(106–126), iii: 1:1 weight ratio between heparin and PrP(106–126), and iv: 5:1 weight ratio between heparin and PrP(106–126).

The transmission electron microscopy (TEM) experiments shown in Figure 5 provide a dramatic visual depiction of the effect of heparin upon the shapes and abundance of the PrP(106–126) fibrils. Figure 5A displays a representative TEM image of a sample of PrP(106–126) incubated with DMPC/DMPG vesicles. The TEM image in Figure 5A shows a crowded network of abundant prion fibrils that appear to "encapsulate" the lighter-complexion phospholipid vesicles. The TEM result in Figure 5B demonstrates the significant inhibitory effect of heparin on vesicle-induced PrP(106–126) fibrillation. Consistently with the other biophysical experiments in Figures 1–4, the 1:1 weight ratio between heparin and PrP(106–126) in Figure 5B was shown to retard fibrillation of the prion peptide significantly. We additionally examined a PrP(106–126)/vesicle/heparin sample in which the heparin/PrP(106–126) weight ratio was *0.2:1* (Figure 5C). Again, consistently with the ThT assay results in Figure 1B indicating enhanced prion fibrillation at such a ratio, the TEM image in Figure 5C features a large number of fibrillar aggregates. However, the shapes of the PrP(106–126) fibrils in Figure 5C, particularly their thickness, appear different from the *lipid-induced* fibers depicted in Figure 5A. Furthermore, in contrast to the packed fibril assemblies that appear closely associated with the DMPC/DMPG vesicles in Figure 5A, the distribution of the fibrils in the presence of heparin (Figure 5C) seems relatively random and distinct from the vesicles. Overall, comparison between the TEM images in Figure 5A (no heparin) and Figure 5B–C (heparin added) supports the conclusion that heparin blocks *lipid-induced* fibrillation of PrP(106–126). Nevertheless, *heparin-induced* fibrillation of PrP(106–126) is promoted in samples containing a *low-weight ratio* between heparin and the prion peptide.[24]

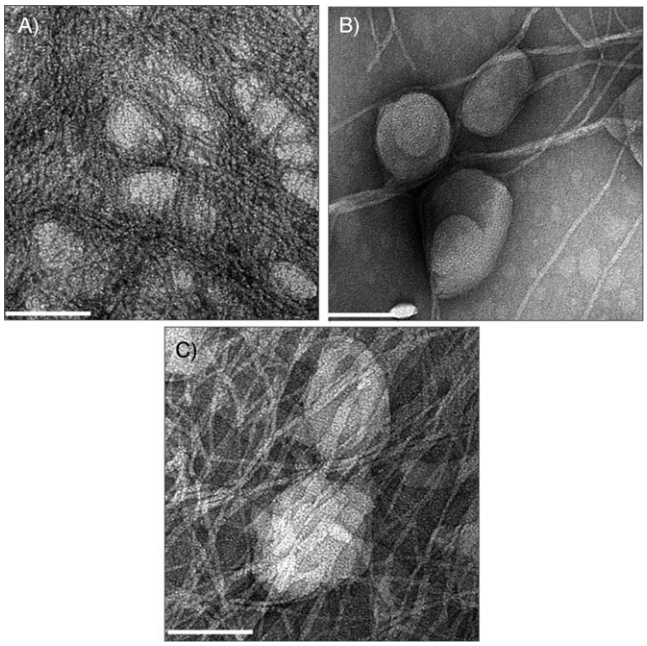

Figure 5. Morphological variations in PrP(106–126) fibrils, depending upon the presence of heparin and the ratio between heparin and the prion peptide. Transmission electron microscopy images of samples consisting of PrP(106–126) and DMPC/DMPG vesicles (1:1 mole ratio): A) PrP(106–126) incubated with the lipid vesicles with no heparin added, B) weight ratio of 1:1 between heparin and PrP(106–126), and C) weight ratio of 0.2:1 between heparin and PrP(106–126). Bars represent 100 nm.

Discussion

Membrane interactions of amyloidogenic proteins appear to play critical roles in the physiology and toxicity encountered in many amyloid diseases. In parallel, glycosaminoglycans have been also shown in many instances to modulate amyloidogen-

esis and toxicity. Although the *separate, distinct effects* either of membranes or of GAGs upon fibrillation processes of amyloid proteins have been extensively assessed, investigations of the *relationship* between GAGs and membranes as factors affecting amyloid protein properties have been rare. This study provides a framework for elucidating the effects of heparin on membrane interactions of an amyloidogenic peptide determinant of the prion protein, revealing pronounced interference by heparin in the interactions of the peptide with phospholipid bilayers and its lipid-induced fibrillation processes.

The experimental data presented indicate that the electrostatic attraction between PrP(106–126) and heparin predominates over the affinity of the peptide towards negatively charged phospholipids in membrane bilayers (Figure 2). Importantly, even small concentrations of heparin were shown to inhibit membrane interactions of the prion peptide (Figure 3) and dampened lipid-induced fibrillation of PrP(106–126) (Figure 1). The fibrillation kinetics data (Figure 1) and TEM experiments (Figure 5) both underscore another significant result: although heparin appeared to block membrane interactions of PrP(106–126), it *did not* universally eliminate fibrillation of the prion peptide. Rather, in solutions containing low heparin/PrP(106–126) mole ratios, pronounced PrP(106–126) fibril assemblies still formed, although a significant fraction of the aggregates was induced by *heparin* and not by the DMPG/DMPC vesicles.

Indeed, the dependence of PrP(106–126) structural features (Figure 4) and fibrillation properties (Figure 1) on the heparin/PrP(106–126) mole ratios appears highly similar to phenomena encountered in heparin/PrP(106–126) mixtures *not* containing phospholipid vesicles.[24] In such mixtures it was hypothesized that the negatively charged heparin surface constituted either a scaffolding for fiber nucleation in solutions with *low abundance* of heparin, or a fibrillation inhibitor through electrostatic binding in cases of *high* heparin/PrP(106–126) mole ratios.[24]

The schematic drawing depicted in Figure 6 summarizes our findings. In solutions containing *just* vesicles (no heparin), PrP(106–126) interacts with the negatively charged phospholipids at the vesicle surface through electrostatic interactions, rapidly forming fibrillar assemblies (Figure 6 A). However, when heparin is present in the vesicle solution, the electrostatic attraction between PrP(106–126) and heparin is the dominant factor, effectively blocking membrane interactions of the peptide, resulting in heparin-induced fiber formation (in samples with *low* heparin/prion ratios, Figure 6 B), or leading to no fibrillation (in samples with *high* heparin/prion ratios, Figure 6 C).

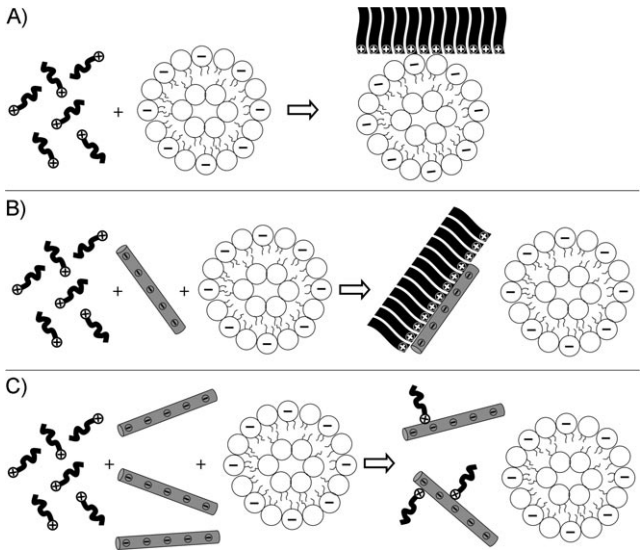

Figure 6. Schematic model for the effects of phospholipid vesicles and heparin on membrane interactions and fibrillation of PrP(106–126). A) No heparin present: the prion peptide (black) binds to the DMPC/DMPG vesicles, which catalyze the formation of fibril assemblies. B) In the presence of relatively *low concentrations* of heparin (gray rod), binding of PrP(106–126) to the vesicles is inhibited and fibrils are formed upon the heparin scaffolding. C) In the presence of relatively *high concentrations* of heparin, binding of PrP(106–126) to the vesicles is similarly blocked, but no fibrils are formed because the prion peptides are bound to individual heparin units through electrostatic attraction.[23]

Conclusions

In conclusion, this work provides evidence that heparin interferes with membrane interactions of the prion amyloidogenic determinant, rather than disrupting the peptide fibrillation process. This outcome is the likely factor accounting for the antitoxic activity of heparin in particular and of GAGs in general, because the toxicities of many amyloid proteins have been traced to the biological action of membrane-active oligomeric species. The ability of heparin to detach lipid-bound prion fragments from the membrane surface emphasizes its therapeutic potential. Our results suggest that tuning of GAG concentrations might be an effective strategy for overcoming the adverse physiological effects of amyloid protein systems—resulting in inhibition of membrane interactions of amyloid species.

Experimental Section

Materials: PrP(106–126) was purchased from GL Biochem (Shanghai, China) in a lyophilized form at $>95\,\%$ purity (HPLC). Heparin (sodium salt) from porcine intestine was purchased from Sigma–Aldrich. 1,2-Dimyristoyl-*sn*-glycero-3-phosphocholine (DMPC), 1,2-dimyristoyl-*sn*-glycero-3-[phospho-*rac*-(1-glycerol)] (DMPG), 1,2-dimyristoyl-*sn*-glycero-3-phosphoethanolamine-*N*-(7-nitro-2–1,3-benzoxadiazol-4-yl) (*N*-NBD-PE) and 1,2-dimyristoyl-*sn*-glycero-3-phosphoethanolamine-*N*-(lissamine rhodamine B sulfonyl) (N-Rh-PE) were purchased from Avanti Polar Lipids (AL).

Vesicle preparation: Vesicles consisting of DMPC and DMPG were prepared by dissolving the lipid components in chloroform/ethanol (1:1, *v*/*v*) and drying together in vacuo. Small unilamellar vesicles (SUVs; DMPC and DMPC/DMPG 1:1, mole ratio) were prepared in Tris base (pH 7.4) by probe-sonication of the aqueous lipid mixtures at room temperature for 10 min. Vesicle suspensions were allowed to anneal for 1 h at room temperature prior to usage. For all experiments except monolayer adsorption, final lipid concentrations were 0.5 mM in Tris buffer (pH 7.4, 5 mM).

PrP(106–126) samples: The following protocol was carried out for the ThT fluorescence and circular dichroism experiments: stock

peptide solutions were prepared by dissolving lyophilized peptide in H_2SO_4 (10 mM) up to a final concentration of 1.5 mM. Acidic conditions were applied to prevent peptide aggregation. Aliquots of the stock solution were either used immediately or were stored at −80 °C for up to two weeks. Before measurements, the PrP(106–126) stock solutions were neutralized with NaOH. For transmission electron microscopy, adsorption isotherms, and fluorescence resonance energy transfer experiments, stock peptide solutions were prepared by dissolving lyophilized peptide in DMSO. For all experiments except adsorption isotherms, the final PrP(106–126) concentrations were 50 μM and the desired weight ratios of peptide to heparin were used.

Thioflavin T (ThT) fluorescence: ThT fluorescence measurements were conducted at 25 °C with a Varioskan (Thermo, Finland) instrument and use of multiwell path cell culture plates. ThT concentrations of 10 μM were used in 240 μL solutions. Measurements of samples containing DMPC/DMPG lipid vesicles and different PrP(106–126)/heparin mole ratios were conducted simultaneously. The device was programmed to record fluorescence intensity every minute for the initial 2.5 h and every 30 min for the remaining few hours. Excitation and emission wavelengths were 445 nm and 485 nm, respectively. The fluorescence curves were smoothed by a five-point adjacent averaging technique. Single exponential functions were fitted to the kinetic plots reporting the measured ThT fluorescence versus time in order to determine the aggregation rate constants (k_{agg}).[36]

Circular dichroism (CD): Solutions (300 μL) composed of lipid vesicles, PrP(106–126), and heparin at different mole ratios were incubated for 30 min at 25 °C without agitation before analysis. CD signals resulting from buffer containing H_2SO_4, NaOH, DMPC or DMPC/DMPG vesicles, and the corresponding concentration of heparin were subtracted from the spectrum of each peptide sample. Measurements were carried out with a Jasco-815 CD spectropolarimeter. Spectra were obtained between 190–260 nm in a quartz cell of 1.0 mm path length, with a 10 nm min^{-1} scan speed. Data were automatically converted into ellipticity (θ in deg cm^2 dmol^{-1}) according to Equation (1):

$$[\theta] = \Psi/(1000\,nlc) \quad (1)$$

where Ψ is the CD signal in degrees, n is the number of peptide bonds, l is the path length in centimeters, and c is the concentration in dmol cm^{-3}. The CD spectra were smoothed by use of a 15-point adjacent averaging procedure.

Transmission electron microscope (TEM): Samples (30 μL) of DMPC/DMPG lipid vesicles, PrP(106–126), and heparin were incubated for 3 h at 25 °C without shaking. Aliquots (5 μL) were placed on 400-mesh copper grids covered with a carbon-stabilized Formvar film. Excess solution was removed after a two-minute incubation, and the grids were negatively stained for one minute with uranyl acetate solution (1%). Samples were viewed with a JEOL 1200EX electron microscope operating at 120 KV.

Fluorescence resonance energy transfer (FRET): Lipid vesicles were prepared by the procedure described above. Prior to drying, the lipid vesicles were additionally supplemented with N-NBD-PE and N-Rh-PE at a 200:1:1 mole ratio (phospholipids/N-NBD-PE/N-Rh-PE). Aliquots (30 μL) of DMPC/DMPG lipid vesicles and different PrP(106–126)/heparin mole ratios were withdrawn after 3 h incubation at 25 °C and diluted in deionized water to a final volume of 200 μL. Fluorescence emission spectra were acquired (excitation 469 nm) in the range of 500–650 nm with a Varioskan (Thermo, Finland) instrument and multiwell path cell culture plates. The percentage of FRET efficiency was determined by Equation (2):

$$\text{FRET efficiency} = [(R_i - R_{Triton})/(R_{Control} - R_{Triton})] - 1 \quad (2)$$

where R is the ratio of N-Rh-PE fluorescence emissions (590 nm)/NBD-PE (536 nm), R_i corresponds to the peptide/vesicle mixtures, R_{Triton} was measured after the addition of Triton X-100 (10%) to the vesicles (Triton X-100 is a detergent causing complete dissociation of the vesicles), and $R_{Control}$ corresponds to vesicles without any additives.

Adsorption isotherms: The experiments were performed at 25 °C with a Nima 312D Teflon trough (Nima Technology Ltd., Coventry, UK). The adsorption isotherms ($\Delta\pi$ vs. time) were monitored throughout the duration of the experiment with the aid of a Nima PS4 Wilhelmy plate sensor. Lipid monolayers consisting of DMPC/DMPG (1:1, mole ratio) at 7 mN m^{-1} were formed by deposition of the lipid solutions at the air/water interface of the dipping well (total volume of 50 mL). After 15 min of solvent evaporation and equilibration, gentle stirring was applied and the peptide or heparin were injected into the water subphase below the preformed lipid monolayer through a thin, vertical tube. The final concentration of the peptide was 0.5 μM. Heparin was either injected into the subphase before the peptide to a final concentration of 0.005 mg mL^{-1} (5:1, *w/w*) or added 90 min after the peptide had been injected into the subphase to a final concentration of 0.0125 mg mL^{-1}.

Acknowledgements

We are grateful to the Germany-Israel DIP Foundation for generous financial support.

Keywords: amyloid peptides · heparin · inhibition · membrane interactions · prions

[1] S. J. DeArmond, S. B. Prusiner, *Am. J. Pathol.* **1995**, *146*, 785–811.
[2] S. B. Prusiner, *Proc. Natl. Acad. Sci. USA* **1998**, *95*, 13363–13383.
[3] P. J. Peters, A. Mironov, Jr., D. Peretz, E. van Donselaar, E. Leclerc, S. Erpel, S. J. DeArmond, D. R. Burton, R. A. Williamson, M. Vey, S. B. Prusiner, *J. Cell. Biol.* **2003**, *162*, 703–717.
[4] B. Fevrier, D. Vilette, F. Archer, D. Loew, W. Faigle, M. Vidal, H. Laude, G. Raposo, *Proc. Natl. Acad. Sci. USA* **2004**, *101*, 9683–9688.
[5] N. Naslavsky, R. Stein, A. Yanai, G. Friedlander, A. Taraboulos, *J. Biol. Chem.* **1997**, *272*, 6324–6331.
[6] N. Sanghera, T. J. Pinheiro, *J. Mol. Biol.* **2002**, *315*, 1241–1256.
[7] M. F. Engel, *Chem. Phys. Lipids* **2009**, *160*, 1–10.
[8] S. Florent-Bechard, C. Desbene, P. Garcia, A. Allouche, I. Youssef, M. C. Escanye, V. Koziel, M. Hanse, C. Malaplate-Armand, C. Stenger, B. Kriem, F. T. Yen-Potin, J. L. Olivier, T. Pillot, T. Oster, *Biochimie* **2009**, *91*, 804–809.
[9] G. P. Gorbenko, P. K. Kinnunen, *Chem. Phys. Lipids* **2006**, *141*, 72–82.
[10] P. K. J. Kinnunen, *The Open Biology Journal* **2009**, *2*, 163–175.
[11] J. Kazlauskaite, N. Sanghera, I. Sylvester, C. Vénien-Bryan, T. J. T. Pinheiro, *Biochemistry* **2003**, *42*, 3295–3304.
[12] A. Linker, H. C. Carney, *Lab. Invest.* **1987**, *57*, 297–305.
[13] A. D. Snow, H. Mar, D. Nochlin, K. Kimata, M. Kato, S. Suzuki, J. Hassell, T. N. Wight, *Am. J. Pathol.* **1988**, *133*, 456–463.
[14] A. D. Snow, J. Willmer, R. Kisilevsky, *Lab. Invest.* **1987**, *56*, 120–123.
[15] O. Ben-Zaken, S. Tzaban, Y. Tal, L. Horonchik, J. D. Esko, I. Vlodavski, A. Taraboulos, *J. Biol. Chem.* **2003**, *278*, 40041–40049.
[16] L. Bergamaschini, E. Rossi, C. Storini, S. Pizzimenti, M. Distaso, C. Perego, A. De Luigi, C. Vergani, M. G. De Simoni, *J. Neurosci.* **2004**, *24*, 4181–4186.

[17] B. Dudas, M. Rose, U. Cornelli, A. Pavlovich, I. Hanin, *Neurodegener. Dis.* **2008**, *5*, 200 – 205.
[18] M. Perez, F. Wandosell, C. Colaco, J. Avila, *Biochem. J.* **1998**, *335*, 369 – 374.
[19] S. J. Pollack, I. I. J. Sadler, S. R. Hawtin, V. J. Tailor, M. S. Shearman, *Neurosci. Lett.* **1995**, *184*, 113 – 116.
[20] A. G. Woods, D. H. Cribbs, E. R. Whittemore, C. W. Cotman, *Brain Res.* **1995**, *697*, 53 – 62.
[21] R. Bravo, M. Arimon, J. J. Valle-Delgado, R. Garcia, N. Durany, S. Castel, M. Cruz, S. Ventura, X. Fernandez-Busquets, *J. Biol. Chem.* **2008**, *283*, 32471 – 32483.
[22] N. Motamedi-Shad, E. Monsellier, S. Torrassa, A. Relini, F. Chiti, *J. Biol. Chem.* **2009**, *284*, 29921 – 29934.
[23] S. Yu, S. Yin, N. Pham, P. Wong, S. C. Kang, R. B. Petersen, C. Li, M. S. Sy, *FEBS J.* **2008**, *275*, 5564 – 5575.
[24] E. Bazar, R. Jelinek, *ChemBioChem* **2010**, *11*, 1997 – 2002.
[25] L. Kupfer, W. Hinrichs, M. H. Groschup, *Curr. Mol. Med.* **2009**, *9*, 826 – 835.
[26] D. R. Brown, B. Schmidt, H. A. Kretzschmar, *Nature* **1996**, *380*, 345 – 347.
[27] G. Forloni, N. Angeretti, R. Chiesa, E. Monzani, M. Salmona, O. Bugiani, F. Tagliavini, *Nature* **1993**, *362*, 543 – 546.
[28] F. Tagliavini, F. Prelli, L. Verga, G. Giaccone, R. Sarma, P. Gorevic, B. Ghetti, F. Passerini, E. Ghibaudi, G. Forloni, *Proc. Natl. Acad. Sci. USA* **1993**, *90*, 9678 – 9682.
[29] J. Dorosz, R. Volinsky, E. Bazar, S. Kolusheva, R. Jelinek, *Langmuir* **2009**, *25*, 12501 – 12506.
[30] T. Miura, M. Yoda, N. Takaku, T. Hirose, H. Takeuchi, *Biochemistry* **2007**, *46*, 11589 – 11597.
[31] I. Dupiereux, W. Zorzi, L. Lins, R. Brasseur, P. Colson, E. Heinen, B. Elmoualij, *Biochem. Biophys. Res. Commun.* **2005**, *331*, 894 – 901.
[32] S. T. Henriques, L. K. Pattenden, M. I. Aguilar, M. A. Castanho, *Biophys. J.* **2008**, *95*, 1877 – 1889.
[33] S. T. Henriques, L. K. Pattenden, M. I. Aguilar, M. A. Castanho, *Biochemistry* **2009**, *48*, 4198 – 4208.
[34] J. I. Kourie, A. Culverson, *J. Neurosci. Res.* **2000**, *62*, 120 – 133.
[35] M. Salmona, G. Forloni, L. Diomede, M. Algeri, L. De Gioia, N. Angeretti, G. Giaccone, F. Tagliavini, O. Bugiani, *Neurobiol. Dis.* **1997**, *4*, 47 – 57.
[36] H. Naiki, K. Higuchi, M. Hosokawa, T. Takeda, *Anal. Biochem.* **1989**, *177*, 244 – 249.
[37] M. Calamai, J. R. Kumita, J. Mifsud, C. Parrini, M. Ramazzotti, G. Ramponi, N. Taddei, F. Chiti, C. M. Dobson, *Biochemistry* **2006**, *45*, 12806 – 12815.
[38] R. Maget-Dana, *Biochim. Biophys. Acta Biomembr.* **1999**, *1462*, 109 – 140.
[39] V. Vie, N. Van Mau, L. Chaloin, E. Lesniewska, C. Le Grimellec, F. Heitz, *Biophys. J.* **2000**, *78*, 846 – 856.
[40] L. M. S. Loura, R. F. M. de Almeida, M. Prieto, *J. Fluoresc.* **2001**, *11*, 197 – 209.
[41] L. M. Loura, A. Coutinho, A. Silva, A. Fedorov, M. Prieto, *J. Phys. Chem. B* **2006**, *110*, 8130 – 8141.
[42] A. Shtainfeld, T. Sheynis, R. Jelinek, *Biochemistry* **2010**, *49*, 5299 – 5307.
[43] J. T. Pelton, L. R. McLean, *Anal. Biochem.* **2000**, *277*, 167 – 176.

Received: August 19, 2010
Published online on February 18, 2011

